



ORIGINAL ARTICLE

Medicine Science 2022;11(3):1030-5

## Spatial clustering and hot spot analysis of the COVID-19 pandemic in Malatya province

Fatma Zeren<sup>1</sup>, Sami Akbulut<sup>2</sup>, Ali Ozer<sup>2</sup>, Huseyin Islek<sup>3</sup>,  
 Recep Bentli<sup>4</sup>, Emin Yahya Mentese<sup>5</sup>

<sup>1</sup>Inonu University, Statistics and Econometrics Research and Application Center, Malatya, Turkey

<sup>2</sup>Inonu University Faculty of Medicine, Department of Public Health, Malatya, Turkey

<sup>3</sup>Mus Alparslan University, Faculty of Economics and Administrative Sciences, Department of Economics, Mus, Turkey

<sup>4</sup>Inonu University Faculty of Medicine, Department of Internal Medicine, Malatya, Turkey

<sup>5</sup>Bogazici University, Kandilli Observatory and Earthquake Research Institute, Department of Earthquake Engineering, Istanbul, Turkey

Received 04 May 2022; Accepted 16 June 2022

Available online 20.06.2022 with doi: 10.5455/medscience.2022.05.105

Copyright@Author(s) - Available online at [www.medicinescience.org](http://www.medicinescience.org)

Content of this journal is licensed under a Creative Commons Attribution-NonCommercial 4.0 International License.



### Abstract

It was revealed that what caused the disease that emerged with respiratory symptoms (fever, cough, shortness of breath) towards the end of 2019 in Wuhan city of China's Hubei province, and later named as COVID-19 by WHO was SARS-CoV-2 virus. The COVID-19 epidemic affected Turkey very quickly as it did the entire world, and the first official case in Turkey was detected in March 2020. In this study, how the COVID-19 cases are clustered in the districts of Malatya and the structure of this clustering as well as whether the cluster has changed over time was revealed by using the spatial exploratory analysis approach. For this purpose, Global and Local Moran I statistics that measure spatial interaction were used. For the hot spot analysis, Getis-Ord's  $G_i^*$  statistic was used. Moran I, which measures the spread of COVID-19 among districts, is statistically significant, and the spread effect is close to medium, although not very strong. It has been determined that Yazihan and Akçadağ districts are the riskiest districts on average as of the period under consideration according to Lokal Moran I statistics. According to the Getis-Ord's  $G_i^*$  statistics, Yazihan district is the one that is most suitable for the spread of the epidemic for Malatya, again being a hot spot location. It has been observed that Yazihan district is frequently in the hot spot according to the monthly analysis of the  $G_i^*$  statistics. In this context, it is important for Yazihan district to increase the necessary measures in the coming periods and to make efforts to raise awareness of the citizens.

**Keywords:** COVID-19 pandemic, exploratory spatial data analysis, Malatya province

### Introduction

Throughout history, people have had to fight epidemics that have more devastating effects than wars. In the 21<sup>st</sup> century, SARS-CoV-1 and then MERS-CoV infectious diseases have led to illness and death, first in China and then in the Middle East. The COVID-19 (virus: SARS-CoV-2) infection, which emerged in China at the end of 2019, was not limited to only regional effects like others, but spread all over the world in a short time [1]. As of February 2020, the World Health Organization (WHO) named this contagious disease as the new type of corona virus (SARS-CoV2)

and it was referred to as COVID-19 in the literature [2]. Spreading rapidly all over the world, COVID-19 was declared a pandemic by the WHO on March 11, 2020 [1]. As of April 14, 2022, a total of 500.186.525 cases were detected worldwide, and unfortunately, 6.190.349 people died due to COVID-19 and related complications in this process [3]. In Turkey, 14.775.634 cases were detected and 97.666 people died [4]. Increasing death and case numbers indicate that COVID-19 continues as a public health problem.

This respiratory disease, which spreads rapidly as a result of human interaction, is transmitted through droplets. Therefore, many countries have first resorted to non-pharmaceutical measures to reduce the spread of Covid-19. Among the non-pharmaceutical measures, the social distancing rule comes first. Social distancing rules are known as measures such as online education, working from home, and cancellation of public demonstrations and meetings. The second measure is personal protection such as the

\*Corresponding Author: Sami Akbulut, Inonu University Faculty of Medicine, Department of Surgery, Public Health, Biostatistics and Medical Informatics, Malatya, Turkey, E-mail: [akbulutsami@gmail.com](mailto:akbulutsami@gmail.com)

use of masks and gloves and frequent hand washing. The third one is certain practices such as quarantining the necessary people as a result of filiation (contact tracing) by conducting tests [5]. In the later stages of the epidemic, vaccines were used as an important tool in the fight against Covid-19. However, the increase in the number of cases and deaths with the emergence of new variants places non-pharmaceutical measures in a central place in the fight against Covid-19. Non-pharmaceutical measures, especially those involving spatial restrictions by governments, are not sustainable practices for economic and social reasons. In this context, revealing the spatial dynamics of the epidemic is very important for decision makers for reasons such as preventing and controlling contagion and developing public health policies.

Spatial analysis methods that use geographic information systems are effective methods in investigating the spread of infectious diseases by using space and time data [6]. It is also possible to observe the distribution of the disease in terms of locations with the spatial analysis approach. Spatial analyses according to time intervals, on the other hand, will reveal the scope and effects of the pandemic in a broader framework. Thus, the decision makers will become the route determiners.

There are various studies in the literature to reveal the spatial characteristics of epidemic diseases. Spatial analysis methods were also used in epidemic diseases other than Covid-19. Studies in this framework are available in the literature for H1N1 [7], SARS [8,9], Influenza [10], Lassa fever [11] and Dengue fever [12,13]. The spatial dynamics of the Covid-19 epidemic that is being experienced on a global scale have also been the subject of many studies. There are some important studies in the literature. Kang et al. [14] tried to determine the spatial spread of the Covid-19 epidemic using data from January 16 to February 6, 2020 for 31 regions of China. The results of the study show that there is spatial dispersion with significant Moran I statistics. Huang et al., [15] revealed the spread of the epidemic with spatial statistical analysis using the data for China from January 13 to March 9, 2020. Moran I statistics were found to be significant, and a positive spreading effect emerged. Ghosh and Cartone [16] aimed to determine the spatial characteristics of the epidemic by using the data of Italy from February 24 to June 26, 2020. In the study conducted for the regions and provinces of Italy, it was observed that there were strong spatial clusters. Tuzcu [17] realized the number of COVID-19 cases and deaths for the provinces of Turkey by spatial exploratory analysis. Geographical weight and economic weight matrices are used as spatial weight matrix. It has achieved a high level of spatial autocorrelation. Zhang et al. [18] have tried to determine the spatial dynamics of the epidemic by examining the Covid-19 and SARS epidemic in China with various social and demographic variables. The results of the study have revealed different spatial clusters. Zeren and Yılanç [19] put forward hot spot cities with spatial exploratory analysis approaches in order to reveal the spatial structure of COVID-19 for the provinces of Turkey. Wang et al., [20] have revealed the spatial dynamics of Covid-19 for the USA using data from January 22 to May 13, 2020 in their study. Islam et al. [6] have revealed the spatial pattern of COVID-19 disease regarding Bangladesh in their study using spatial autocorrelation analysis. They examined particularly the regions where the risk of epidemics is high with hot spot analysis. Ning et al. [21] tried to determine the spatial characteristics of the

spread using the daily and total number of Covid-19 cases for 30 regions of China. According to the results of the study, while the total cases show an S-shaped curve, the daily cases show a trend in the form of an increase and then a decrease. In addition, while the density of the distribution of daily and total cases is higher in the eastern regions, it tends to decrease in the west. Fatima et al. [22] conducted a spatial clustering and hot spot analysis by using 2020 Covid-19 data for each country in their study. The results showed that Covid-19 exhibits different clustering characteristics in different months. It has been stated that for the January-April period, the hotspot areas have shifted from the Western Pacific to Europe and America, and the Eastern Mediterranean countries have been under the influence of Covid-19 since July. Also, Africa has remained a cold spot region. Zeren et al. [23] have investigated the spatial relationship between the first 14 days and the next 14 days of the epidemic for 20 regions of Italy. As a result of the study, they obtained a significant Moran I statistic and stated that there was spatial autocorrelation. In addition, it was concluded that the cases that emerged in the first 14 days were effective on the cases in the second 14 days. In their studies, Aral and Bakır [24] have detected the spatial interactions of 81 provinces of Turkey for the time period covering the date range of 8 February and 28 May 2021. In addition, according to the results of spatial regression analysis, it was revealed that population density and elderly dependency ratio were important factors affecting the number of cases. In their study, Hridoy et al. [25] have investigated the spatial variation of Covid-19 for 64 regions in Bangladesh, using the daily case numbers between March 8, 2020 and March 10, 2021. The findings of the study show that there is a high level of positive autocorrelation between population density and Covid-19 contagion. In addition, the study shows that various restriction measures are moderately effective in increasing contagion.

This study aims to determine the spatial clustering of Covid-19 and hot spot areas for Malatya province, one of the metropolitan cities of Turkey. For this purpose, spatial interaction and hot spot analyses will be used. In the second part of this study, spatial analysis methods will be introduced. In the third part, empirical findings will be presented, and in the last part will consist of the conclusion.

## Materials and Methods

### Spatial Interaction Analysis: Moran I and Local Moran I

Tobler's law of geography states that spatial units share more similarities with nearby units than with distant units. This concept is known as spatial dependency. Spatial dependency, on the other hand, refers to the degree of spatial autocorrelation between independently measured values belonging to geographical locations. This autocorrelation arises as a result of greater interaction and information dissemination between locations that are close to each other. The most common of the tests investigating the presence of spatial autocorrelation is the Moran I statistic.

Moran's I statistic is the most widely used indicator of spatial autocorrelation. It was first proposed by Moran [26] in 1948 and was later popularized by Cliff and Ord's [27] classic work on spatial autocorrelation. The level and structure of spatial clustering is measured by this correlation. This statistic for a single variable is as follows [28].

$$(1) \quad I_U = \frac{Y'WY}{n}$$

$Y$  indicates the variable that represents the property of the locations.  $n$  shows the total number of locations or the total number of observations of the  $Y$  variable.  $W$  is the spatial weight matrix that measures  $(n \times n)$  dimensional spatial interactions.  $w_{ij}$  denotes each element of the weight matrix. The value of these elements indicates whether the positions are adjacent or not. In this study, the queen weight matrix was used. This weight matrix defines the neighbourhood according to the boundary sharing, and locations that share a common edge or corner are considered neighbours. Neighbouring observations in the weight matrix are indicated by a value of 1, and non-neighbouring observations are indicated by 0. In applications, the row-level standardized version of the weight matrix ( $\sum w_{ij}=1$ ) is preferred. This matrix was also used in this study. Moran I statistic takes values between -1 and +1. Closer to 1 means that regions with similar values are clustered together, and closer to -1 means that dissimilar values are clustered together.

The univariate Moran I statistic was developed by Anselin et al. [28] to measure the spatial interaction between two different variables. This correlation is called bivariate spatial correlation [28]. It is the correlation between the  $x_i$  variable and the  $y_i \sum_j w_{ij} y_j$  variables with spatial lag. The bivariate Moran I statistic is as follows:

$$(2) \quad I_B = \frac{X'WY}{n}$$

Standardized forms of  $x_i$  and  $y_i$  variables (with zero mean value and 1 if variance values are used) are used here.

The Moran I statistics explained above is a global statistic that gives a single value for all locations. A local version of this statistic is also available and is called Local Moran I.

The local Moran I statistic, proposed by Anselin, [29] measures spatial interaction for each spatial unit or location and is called the Local Indicator of Spatial Association (LISA). It is used to detect local clusters and local spatial deviating values. The local Moran I statistic for a single variable is as follows [29,30].

$$(3) \quad I_i = (y_i - \bar{y}) \sum_{j=1}^n w_{ij} (y_j - \bar{y}) \text{ for } i \neq j$$

LISA statistic is a statistic that measures the similarity of the analysed location with the surrounding locations.

The bivariate Moran I statistic is as follows. It is the spatial correlation between the variable  $x_i$  at position  $i$  and the variables  $y_j$  of its neighbours at this location. That is, it is the correlation between the  $x_i$  and  $\sum_j w_{ij} y_j$  variables.

$$(4) \quad I_i^B = (x_i - \bar{x}) \sum_{j=1}^n w_{ij} (y_j - \bar{y}) \text{ for } i \neq j$$

With the value of the local Moran I statistic, four different spatial structures or patterns can emerge: High-High (HH) and Low-Low (LL) clustering areas and High-Low (HL) and Low-High (LH) deviating value areas. Clustering areas are in the positive correlation category and deviating value areas are in the negative correlation category. Specifically, an HH cluster represents neighbourhoods where the incidence of epidemics is relatively high. The LL cluster, on the other hand, shows neighbourhoods where the incidence of epidemics is relatively low. An HL (LH)

deviating or outlier primarily means that the high (low) value area is surrounded by a low (high) value area.

The significance of both univariate and bivariate Global Moran I and Local Moran I statistics was determined by randomization approach. In this approach, the observed values of the relevant variables are randomly redistributed to the locations, and the statistics are recalculated after each distribution. Thus, the reference distribution of the relevant statistics is obtained.

### Hot spot Analysis

The first statistical theory for local spatial autocorrelation was proposed by Getis et al.[30] later this statistic was further elaborated by Ord and Getis.[31] It is a statistic based on the logic of the point pattern analysis approach. There are two versions of this statistic: Of these, the value of the location of interest with the  $G_i^*$  statistic is taken into account, while the value of the location of interest with the  $G_i$  statistic is ignored. The second one consists of the ratio of the weighted average of values at neighbouring locations to the sum of all values except the value at that location. The first considers the value of the position of interest in both the numerator and the denominator. These statistics are as follows.

$$(5) \quad G_i = \frac{\sum_{i \neq j} w_{ij} x_j}{\sum_{i \neq j} x_j}$$

$$(6) \quad G_i^* = \frac{\sum_j w_{ij} x_j}{\sum_j x_j}$$

The interpretation of Getis-Ord statistics is very simple: a larger-than-average value or a positive value for standardized z-value refers to the hot spot location, and a lower-than-average value or negative z-value refers to the cold spot location. Unlike the Local Moran and Local Geary statistics, the Getis-Ord approach does not consider spatial deviating values. The distributions of these statistics are obtained by conditional random permutation approaches.

### Results

In this research, spatial dynamics of COVID-19 were visualized at the district level in Malatya. Data were obtained from Malatya Provincial Health Directorate. The data in the date range 23.03.2020-01.06.2021 are used. Before initiating the study, ethics committee approval dated 29.03.2022 and numbered 3248 was obtained from Inonu University Health Sciences Non-Interventional Clinical Research Ethics Committee.

The distribution of the total number of cases per ten thousand people in the mentioned date range by districts is shown in Figure 1. As seen in Figure 1, districts in the highest case group are Battalgazi, Darende and Yesilyurt districts, the high number of cases in the second group is in Yazihan and Arapgir districts, the highest number of cases in the third group is in Doğansehir, Hekimhan and Kale districts, the fourth group number of cases is in Akçadağ and Arguvan districts and the lowest number of cases is in Doğanyol, Kuluncak and Pütürge districts. In short, the darkest coloured districts are the districts with the highest number of cases. The lighter colours are the districts with lower cases compared to the highest case numbers. As the colour brightens, the number of cases is gradually decreasing.

The scatter plot of Moran I statistics, one of the spatial correlation

statistics that measures the interaction between districts in terms of the number of COVID-19 cases, is as seen in Figure 2.

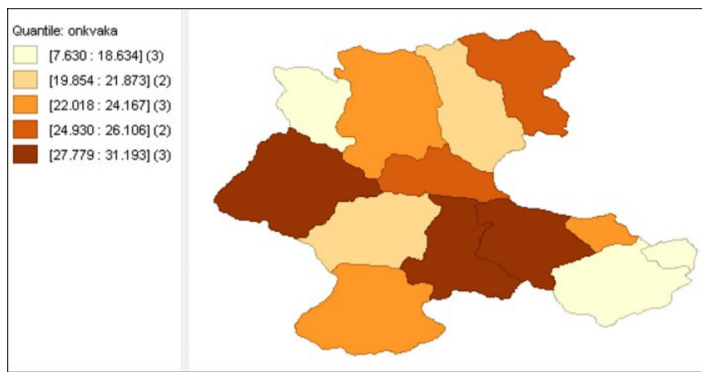


**Figure 1.** Distribution of the total number of cases per ten thousand people by Districts

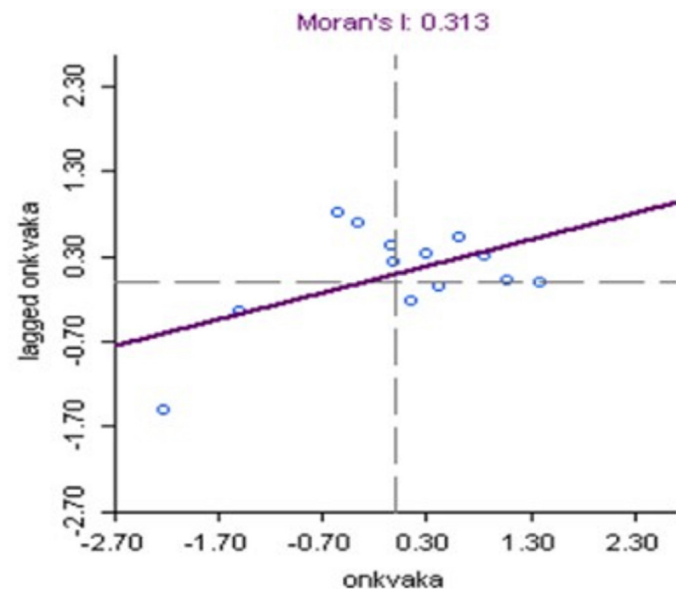


**Figure 2.** Moran I statistics for the total number of cases per ten thousand people

It was found that Moran I statistical value was 0.313, and there was a similarity in terms of the number of cases, but this similarity was not very high and was close to the middle level. One of the reasons for this similarity is that they interact as neighbouring locations. As a result of 999 randomization experiments, the p-value of Moran I statistics is 0.044.

The LISA cluster map for the total number of cases per ten thousand people is shown in Figure 3. As seen in the figure, Yazihan district is the only district with the highest risk in terms of the number of cases, since it is the district in the HH cluster area. In the LH cluster area, there is only Akçadağ district. The LH field is of no significance in the context of the study, as it denotes a deviating value location.

Spatial correlation was also considered in terms of the distribution of cases according to months, and it is seen that Moran I statistics are significant only for April and May. It has been observed that there is a spatial interaction at the district level in these months, but this interaction is not very strong, but close to the medium level. It is as shown in Table 1, which includes Moran I statistics.

It is seen that there is a partial interaction between the districts in

April and May. The results were not reported since the interactions outside of these months were not statistically significant. The cluster map of Getis-Ord  $G_i^*$  statistics for the total number of cases per ten thousand people is as in Figure 4.

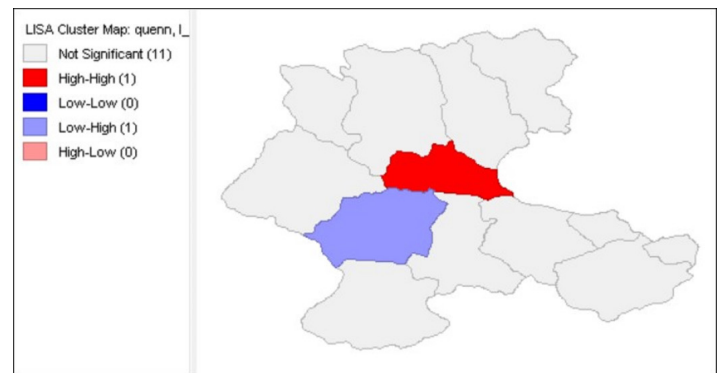


**Figure 3.** LISA cluster map for total cases per ten thousand people

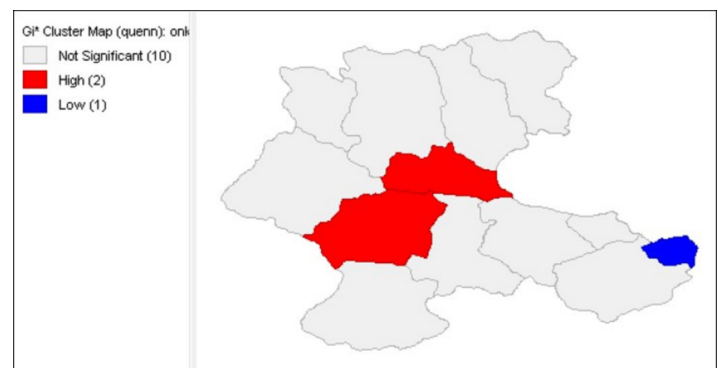


**Figure 4.** Hot spot analysis for total cases per ten thousand people

As seen in this map, Yazihan and Akçadağ districts are hot spot areas, and the cold spot area is Doğanyol district. Doğanyol district, on the other hand, is an area in this position due to the low number of cases. As it is known, hot spot areas are the areas with the highest number of cases and risky areas for the spread of the disease.

**Table 1.** Moran I statistics for cases per ten thousand people by month

Months	Moran I
April	0.248*
May	0.258**

\* Significant for 10% level; \*\* Significant for the 5% level

The Hot Spot analysis results of the number of cases per ten thousand people by months are shown in Table 2.

As can be seen from this table, it has been observed that Yazihan district is often a hot spot area, that is, a risky region with a very high number of cases. Kuluncak, which was a cold spot area in July 2020, turned into a hot spot in October 2020. While it was still a hot spot in December, it turned into a cold spot as of March 2021. Arapgir district, on the other hand, is in the hot spot in May 2021 and January 2021, and in the cold spot in most of the other months. Darende district in April 2020 and Akçadağ district in February 2021 are hot spots. In June 2020 on the other hand, Darende district turned into a cold spot. The fact that Doğanyol district was never a hot spot, but often a cold spot stands out. Arguvan district

is also a cold spot area in April, June 2020 and February 2021. Hot spot areas are the areas where the risk of spreading COVID-19 is greatest. It is therefore important to concentrate measures towards these areas.

**Table 2.** Hot Spot Analysis by Months

Months	Hot Spot	Cold Spot
March (2020)	Arapgir	
April (2020)	Yazihan, darende	Arapgir, Arguvan, Doganyol
June (2020)	-	Arapgir, Arguvan, Darende, Doganyol, Hekimhan, Kuluncak
July (2020)	Yazihan	Doganyol, Kuluncak
August (2020)	-	Arapgir
September (2020)	Yazihan	Doganyol
October (2020)	Kuluncak, Yazihan	Doganyol
November (2020)		Arapgir, Yazihan
December (2020)	Kuluncak, Yazihan	Puturge
January (2021)	Arapgir	Doganyol, Puturge
February (2021)	Akçadag	Arapgir, Arguvan, Darende
March (2021)	Yeşilyurt	Arapgir, Doganyol, Kuluncak
April (2021)	Yazihan	Arapgir, Doganyol
May (2021)	-	Doganyol

## Discussion

In this study, the distribution and spatial structure of COVID-19 in the districts of Malatya were investigated. In general, data between the dates of March 2020 and May 2021 were used. Spatial structure has been revealed within the framework of spatial autocorrelation analysis and hot spot analysis approaches. It has been revealed by the Moran I statistics that in the time period considered globally, there is a spatial interaction, but this interaction is not very strong. Even if the interaction is low, it is very important to keep the possible interaction channels between the districts at a more controllable level in terms of preventing the spread of the disease. According to the results of the local Moran I statistics, the district with the highest risk in terms of spreading or interaction is Yazihan. According to the distribution of the Getis-Ord  $G_i^*$  hot spot analysis in terms of total cases, Yazihan and Akçadağ districts are the riskiest districts in the hot spot position in general. It has been observed that Doğanyol district is in the cold spot location on average as of the period discussed. In the distribution of the hot spot analysis by months, it has been determined that Yazihan district has a high potential for the spread of the virus in April, July, September, October and December in 2020 and in April in 2021. While it was a hot spot in October 2020, it passed the cold spot position in November 2020. However, it was observed that it did not maintain this position and switched to the hot spot position again in December. The data used for the analysis mostly belong to the year 2020, so the detailed results for the year 2020 have emerged more prominently.

## Conclusion

According to the results obtained, intensifying the necessary measures for Yazihan district is required in terms of the course

of COVID-19 in the coming days. It is seen that Arapgir district, on the other hand, is mostly in the cold spot location with low interaction with its neighbours. Of course, this situation is also an indicator of a result related to the geographical location of Arapgir district. Doğanyol, Hekimhan and Arguvan districts are only ones included in the cold spot cluster.

## Conflict of interests

The authors declare that there is no conflict of interest in the study.

## Financial Disclosure

The authors declare that they have received no financial support for the study.

## Ethical approval

Ethics committee approval was obtained from Inonu University institutional review board (IRB) for non-interventional studies (Approval No: 2022/ 3248) and performed according to the ethical (Declaration of Helsinki) and legal standards in Turkey

## References

- Sahin TT, Akbulut S, Yilmaz S. COVID-19 pandemic: Its impact on liver disease and liver transplantation. *World J Gastroenterol.* 2020;26:2987-99.
- Lai CC, Shih TP, Ko WC, et al. Severe acute respiratory syndrome coronavirus 2 (SARS-CoV-2) and coronavirus disease-2019 (COVID-19): The epidemic and the challenges. *Int J Antimicrob Agents.* 2020;55:105924.
- Organization WH: WHO Coronavirus (COVID-19) Dashboard. <https://covid19.who.int/> access data 2022
- Health TMO: Turkish Ministry of Health COVID-19 Information Platform. <https://covid19.saglik.gov.tr>. accesse date 15,7,2022
- Alvi MM, Sivasankaran S, Singh M. Pharmacological and non-pharmacological efforts at prevention, mitigation, and treatment for COVID-19. *J Drug Target.* 2020;28:742-54.
- Islam A, Sayeed MA, Rahman MK, et al. Geospatial dynamics of COVID-19 clusters and hotspots in Bangladesh. *Transboundary and Emerg Dis.* 2021;68:3643-57.
- Lee SS, Wong NS. The clustering and transmission dynamics of pandemic influenza A (H1N1) 2009 cases in Hong Kong. *J Infect.* 2011;63:274-80.
- Meng B, Wang J, Liu J, et al. Understanding the spatial diffusion process of severe acute respiratory syndrome in Beijing. *Public Health.* 2005;119:1080-7.
- Fang LQ, de Vlas SJ, Feng D, et al. Geographical spread of SARS in mainland China. *Trop Med Int Health.* 2009;14:14-20.
- Malcolm BL. The spread process of epidemic influenza in the continental United States, 1968–2008. *Spatial and spatio-temporal epidemiology.* 2014;8:35-45.
- Olugasa BO, Dogba JB, Ogunro B, et al. The rubber plantation environment and Lassa fever epidemics in Liberia, 2008–2012: A spatial regression. *Spat Spatiotemporal Epidemiol.* 2014;11:163-74.
- Hafeez S, Amin M, Munir BA. Spatial mapping of temporal risk to improve prevention measures: A case study of dengue epidemic in Lahore. *Spatial and spatio-temporal epidemiology.* 2017;21:77-85.
- Dhewantara PW, Marina R, Puspita T, et al. Spatial and temporal variation of dengue incidence in the island of Bali, Indonesia: An ecological study. *Travel Med Infect Dis.* 2019:101437.
- Kang D, Choi H, Kim J-H, Choi J. Spatial epidemic dynamics of the COVID-19 outbreak in China. *Int J Infect Dis.* 2020;94:96-102.
- Huang R, Liu M, Ding Y. Spatial-temporal distribution of COVID-19 in China and its prediction: A data-driven modeling analysis. *J Infect Dev Ctries.* 2020;14:246-53.
- Ghosh P, Cartone A. A Spatio-temporal analysis of COVID-19 outbreak in Italy. *Regional Science Policy Practice.* 2020;12:1047-62.
- Tuzcu SE. A Spatial Exploratory Look to Covid-19 Cases and Deaths in Turkey. In: Usupbeyli A, editor. *Quantitative Approaches to Current Issues in Economics.* Ankara: Ekin Kitabevi; 2020.p.119-46.

18. Zhang X, Rao H, Wu Y, et al. Comparison of spatiotemporal characteristics of the COVID-19 and SARS outbreaks in mainland China. *BMC Infect Dis.* 2020;20:805.
19. Zeren F, Yilanci V. [Analysing Spatial Patterns of the COVID-19 Outbreak in Turkey]. *Bingol University J Economics Administrative Sci.* 2020;4:27-40.
20. Wang Y, Liu Y, Struthers J, Lian M. Spatiotemporal characteristics of the COVID-19 epidemic in the United States. *Clin Infect Dis.* 2021;72:643-51.
21. Ning J, Chu Y, Liu X, et al. Spatio-temporal characteristics and control strategies in the early period of COVID-19 spread: a case study of the mainland China. *Environ Sci Pollut Res Int.* 2021;28:48298-311.
22. Fatima M, Arshad S, Butt I, Arshad S. Geospatial Clustering and Hotspot Detection of Covid-19 Incidence in 2020: A Global Analysis. *International J Geospatial Environmental Research.* 2021;8:4.
23. Zeren F, Yilanci V, Islek H. [Covid-19 Spread In Regions Of Italy: Exploratory Spatial Data Analysis]. *Electronic J Social Science.* 2021;20:1432-42.
24. Aral N, Bakir H. Spatiotemporal Analysis of Covid-19 in Turkey. *Sustain Cities Soc.* 2022;76:103421.
25. Hridoy A-EE, Tipo IH, Sami M, et al. Spatio-temporal estimation of basic and effective reproduction number of COVID-19 and post-lockdown transmissibility in Bangladesh. *Spatial Information Research.* 2022;30:23-35.
26. Moran PA. The interpretation of statistical maps. *J Royal Statistical Society Series B (Methodological).* 1948;10:243-51.
27. Cliff AD, Ord JK. *Spatial autocorrelation.* London: Pion, 1973;1-178.
28. Anselin L, Syabri I, Smirnov O. *Visualizing multivariate spatial correlation with dynamically linked windows.* Proceedings, CSISS Workshop on New Tools for Spatial Data Analysis, Santa Barbara, CA: Citeseer; 2002.
29. Anselin L. Local indicators of spatial association—LISA. *Geographical Analysis.* 1995;27:93-115.
30. Getis A, Ord JK. The Analysis of Spatial Association by Use of Distance Statistics. *Geographical Analysis.* 1992;24:189-206.
31. Ord JK, Getis A. Local Spatial Autocorrelation Statistics: Distributional Issues and an Application. *Geographical Analysis.* 1995;27:286-306.